

The Hedgehog receptor Patched controls lymphoid lineage commitment

Anja Uhmann,¹ Kai Dittmann,² Frauke Nitzki,¹ Ralf Dressel,² Milena Koleva,¹ Anke Frommhold,¹ Arne Zibat,¹ Claudia Binder,³ Ibrahim Adham,¹ Mirko Nitsche,⁴ Tanja Heller,⁵ Victor Armstrong,⁵ Walter Schulz-Schaeffer,⁶ Jürgen Wienands,² and Heidi Hahn¹

¹Institute of Human Genetics, ²Department of Cellular and Molecular Immunology, ³Department of Haematology and Oncology, ⁴Department of Radiation Therapy and Oncology, ⁵Department of Clinical Chemistry, and ⁶Department of Neuropathology, Georg August University of Göttingen, Göttingen, Germany

A first step in hematopoiesis is the specification of the lymphoid and myeloid lineages from multipotent progenitor cells in the bone marrow. Using a conditional ablation strategy in adult mice, we show that this differentiation step requires Patched (Ptch), the cell surface-bound receptor for Hedgehog (Hh). In the absence of Ptch, the development of T- and

B-lymphoid lineages is blocked at the level of the common lymphoid progenitor in the bone marrow. Consequently, the generation of peripheral T and B cells is abrogated. Cells of the myeloid lineage develop normally in *Ptch* mutant mice. Finally, adoptive transfer experiments identified the stromal cell compartment as a critical Ptch-dependent inducer of

lymphoid versus myeloid lineage commitment. Our data show that Ptch acts as a master switch for proper diversification of hematopoietic stem cells in the adult organism. (Blood. 2007;110:1814-1823)

© 2007 by The American Society of Hematology

Introduction

Hematopoietic stem cells (HSCs) represent the common origin of all cell types within the immune system. According to the Akashi-Kondo-Weissman model, an early event of adult hematopoiesis is the differentiation of multipotent progenitors (MPPs) in the bone marrow (BM) into common myeloid progenitors (CMPs) and common lymphoid progenitors (CLPs).¹⁻³ CMPs further differentiate into megakaryocyte/erythrocyte progenitors (MEPs), or into granulocyte/macrophage progenitors (GMPs), which give rise to megakaryocytes and erythrocytes, or to granulocytes and macrophages, respectively. CLPs develop into precursor B cells, early thymic T-cell progenitors (ETPs), and natural killer (NK) cells.

Discrete developmental stages of myelo- and lymphopoiesis have been defined based on the expression of stage-specific marker proteins (reviewed in Busslinger⁴). For example, HSCs normally express high levels of the surface receptors c-kit and Sca-1, which are both down-regulated as HSCs progress to CLPs. Formation of CLPs requires the transcription factors Spi-1/PU.1 and Ikaros together with the Fms-like receptor tyrosine kinase 3 (Flt3) and the α -chain of the IL-7 receptor (IL-7R α). However, the details of early HSC differentiation are unclear, especially the specification of myeloid and lymphoid precursor cells. Recently, members of the Hedgehog (Hh) family of secreted signaling proteins have been shown to affect the proliferation of primitive hematopoietic cord blood cells^{5,6} and to play a role in proliferation, survival, and differentiation of early T cells and germinal center B cells.^{5,7-11} How Hh affects T-cell development is unclear. The impact of this pathway on B-cell development and the specification of the myeloid lineage has not yet been investigated.

Three mammalian Hh proteins exist (Sonic, Indian, and Desert Hh), which are recognized and bound by the cell surface receptor Patched (Ptch). Binding of Hh to Ptch suspends the inhibition of its membrane-bound signaling partner Smoothed (Smo), which in

turn initiates nuclear translocation and activation of the Gli family of transcription factors. This is followed by the expression of a plethora of downstream target genes including *Bcl-2*, cell-cycle regulators, and *Ptch* itself (reviewed in Ruiz i Altaba et al¹²). Hh/Ptch signaling is critical for cell-fate determination during embryogenesis and for cell growth and differentiation in the adult organism. An abnormal activation of the Hh/Ptch pathway results in developmental abnormalities and tumorigenesis.^{12,13} Because targeted disruption of either Hh or Ptch is embryonically lethal,¹⁴⁻¹⁶ analysis of Hh/Ptch signaling in adult tissues has been largely limited to in vitro analysis. By inducibly abrogating Ptch expression in the mouse, we show here that Hh/Ptch signaling in stromal cells is mandatory for the specification of both B- and T-cell lineages at the CLP progenitor stage, but not of the myeloid lineage in the BM.

Materials and methods

Ptch^{fllox/fllox} and *Ptch*^{fllox/fllox}ERT2^{+/-} mouse line generation

Genomic DNA clones were isolated as described in Hahn et al.¹⁶ To generate the *Ptch*^{fllox} conditional mouse line, a targeting vector derived from pPNT4 described by Conrad et al¹⁷ was constructed, in which a *loxP* site was inserted into intron 7 of the *Ptch* gene. The second *loxP* site together with the *neo*-cassette of the pPNT4 vector was introduced into intron 9. The neomycin resistance cassette of pPNT4 is also flanked by *frt* sites to enable *FLPe* recombinase-mediated excision, if required.¹⁸ The linearized targeting vector was electroporated into R1 embryonic stem cells.¹⁹ Upon positive and negative selection of the transfectants,²⁰ *XhoI*-digested genomic DNA was analyzed by Southern hybridization using a 5' external probe to detect homologous recombination, which was confirmed by polymerase chain reaction (PCR) using the primers Neo-R/p910F.4, Neo-F/p1011R.2, or p910F.4/p1011R.2. Three positive clones were microinjected into

Submitted February 21, 2007; accepted May 23, 2007. Prepublished online as *Blood* First Edition paper, May 29, 2007; DOI 10.1182/blood-2007-02-075648.

The publication costs of this article were defrayed in part by page charge

payment. Therefore, and solely to indicate this fact, this article is hereby marked "advertisement" in accordance with 18 USC section 1734.

© 2007 by The American Society of Hematology

C57BL/6 blastocysts, and obtained chimeric mice were mated to C57BL/6 females. The *agouti* offspring were tested by PCR and Southern blot analysis to confirm germ-line transmission of the *PtcH^{lox}* conditional allele. *PtcH^{lox/+}* siblings were intercrossed to generate *PtcH^{lox/lox}* offspring. The *Rosa26CreERT2* (*ERT2*) knock-in mouse strain (kindly provided by Dr Anton Berns, The Netherlands Cancer Institute, Amsterdam, The Netherlands) expresses a fusion gene encoding Cre recombinase and a modified ligand-binding domain for the estrogen receptor under control of the endogenous *Rosa26* promoter (A. Berns, written personal communication, February 15, 2005). These mice were bred to *PtcH^{lox/lox}* mice. The resulting *PtcH^{lox/+}ERT2^{+/-}* mice were crossed with *PtcH^{lox/lox}* mice to obtain *PtcH^{lox/lox}ERT2^{+/-}* mice. Eight-week-old *PtcH^{lox/lox}ERT2^{+/-}* mice were injected intraperitoneally with 1 mg tamoxifen dissolved in a 1:10 ethanol-sunflower oil emulsion²¹ on 5 consecutive days to induce the *PtcH^{del}* mutation (named *tPtcH^{-/-}* mice) or with solvent alone. Mice with *PtcH^{lox/lox}ERT2^{-/-}* genotypes were used to assess any unspecific effects of tamoxifen. To detect the Cre-mediated *PtcH^{del}* mutation, which removes the floxed exons 8 and 9, mice were genotyped by PCR using the primer combination Exon7-F/NeoR or Neo-F/p1011R.2. For location of primers, see Figure 1A. All experiments using animals were performed according to legal requirements.

Detection and quantification of CreERT2-mediated recombination at the *PtcH^{lox}* locus

Two tamoxifen-treated *PtcH^{lox/lox}ERT2^{+/-}* mice were killed at day 10 after the first injection and genomic DNA was isolated from several organs. *PtcH^{lox/lox}ERT2^{-/-}* mice were used for generation of standard curves. Recombination efficiency was quantified on an ABI PRISM 7900 sequence detection system (Applied Biosystems, Foster City, CA) by real-time PCR using forward primers hybridizing to intron 7 and intron 9, and a common reverse primer hybridizing immediately downstream of the second *loxP* site in intron 9. A FAM-labeled probe was used for detection of the deleted *PtcH^{del}* allele, whereas a Yakima Yellow-labeled probe detected the *PtcH^{lox}* allele. A *pelota* gene-specific quantitative PCR assay was used for data normalization. Data were processed using the standard curve method for relative quantification. Separate standard curves were generated for each tissue. The deletion efficiency was calculated as the ratio of the values for the deleted allele to the total value from a *PtcH^{lox/lox}* mouse plus the deleted allele, and is expressed in percentage. All sequences of primers and probes together with detailed protocols are available upon request.

RNA isolation and reverse-transcription PCR

Total RNA was extracted from various tissues and embryos using TRIZOL reagent (Invitrogen, Carlsbad, CA). Reverse transcription was conducted with random hexamers and SuperScriptII reverse transcriptase (Invitrogen). PCR fragments detecting transcripts derived from *PtcH^{lox}* and *PtcH^{del}* alleles were amplified using the primers mPtc11 and mPtc7R, purified, and sequenced. Amplification of *Gapd* served as control. Primers for amplification of β -actin, *EBF*, *Flt3*, *Ikaros*, *IL-7R α* , *PU.1*, *Rag-1*, and *Rag-2* have been described in DeKoter et al.²² *Gli* transcripts were analyzed using primer pairs specific for *Gli1*, *Gli2*, and *Gli3*. All primer sequences are available upon request.

Blood and BM-cell analysis

Peripheral blood or single-cell suspensions of BM cells derived from femur and tibia of hind limbs as well as thymocytes and splenocytes were prepared and incubated for 15 minutes on ice with different combinations of the following antibodies: anti-CD3-FITC, anti-CD4-biotin, anti-CD8 α -PE, anti-CD8 α -PE-Cy7, anti-CD21-FITC, anti-CD24-PE, anti-CD25-FITC, anti-CD43-biotin, anti-CD44-PE-Cy5, anti-CD45R/B220-PE-Cy7, anti-IgD-FITC, anti-TCR β -FITC (BD Biosciences Pharmingen, San Jose, CA), and anti-IgM-RPE (Southern Biotechnology Associates, Birmingham, AL). Binding of biotinylated antibodies was monitored by streptavidin-PE or streptavidin-PE-Cy7 (BD Biosciences Pharmingen) or by streptavidin-FITC (Southern Biotechnology Associates). Erythrocytes of peripheral blood samples were lysed with fluorescence-activated cell sorting (FACS)

analysis solution (BD Biosciences Pharmingen). Annexin V-PE staining was carried out using an annexin V-PE apoptosis detection kit (BD Biosciences Pharmingen). Hematopoietic stem and progenitor cells from 10⁷ BM cells were purified by depletion of lineage-positive (Lin⁺) cells using the EasySep mouse hematopoietic progenitor cell enrichment kit (StemCell Technologies, Vancouver, BC; depletion kit contains monoclonal antibodies toward murine CD5, B220, Mac-1, Gr-1, Ter119, and 7-4). Enriched lineage-negative (Lin⁻) BM cells were incubated for 15 minutes on ice with anti-CD117 (c-kit)-Biotin, anti-CD127 (IL-7R α)-PE, and anti-Sca-1-FITC, and in a second staining step with streptavidin-PE-Cy7 or streptavidin-PE-Cy5 (all from BD Biosciences Pharmingen). For cell-cycle analysis, 100 μ L of 10 mg/mL BrdU were injected intraperitoneally 3 hours before killing of the mice, and enriched Lin⁻ BM cells were stained with anti-c-kit-Biotin (streptavidin-PE-Cy7), anti-Sca-1-biotin (streptavidin-PE), anti-BrdU-FITC, and 7-AAD (BD BrdU FITC Flow Kit; BD Biosciences Pharmingen). To avoid cross-reactions of unbound biotin binding sites in the biotin/streptavidin complexes, anti-c-kit-biotin and anti-Sca-1-biotin were mixed in separate reactions with the respective streptavidin conjugates that were used in excess. Probes were stained first for c-kit with anti-c-kit-biotin/streptavidin-PE-Cy7 and after extensive washing with anti-sca-1-biotin/streptavidin-PE. Cells were analyzed on an LSR II flow cytometer (BD Biosciences Pharmingen). Data acquisition and analysis were performed using software BD FACS Diva (BD Biosciences Pharmingen) and FlowJo (TreeStar, Ashland, OR), respectively. EDTA blood samples were collected by heart puncture and analyzed on an AcT 5 hematology analyzer (Beckman Coulter, Hialeah, FL) and by blood smear tests.

Clonogenic progenitor assay

Mouse clonogenic progenitor assays were performed by plating 2 \times 10³ Lin⁻ BM cells into a methylcellulose medium (MethoCult 3434; StemCell Technologies) containing SCF, IL-3, IL-6, and Epo according to the manufacturer's instructions. Differential colony counts were scored after 8 days by morphologic characteristics using an inverted microscope. *ERT2*-mediated *PtcH* inactivation in CFU colonies was analyzed by PCR as described in "Detection and quantification of CreERT2-mediated recombination at the *PtcH^{lox}* locus."

Adoptive transfer and repopulation assay

BMs were isolated from control and *tPtcH^{-/-}* mice 19 days after tamoxifen injection and Lin⁻ BM cells were purified as described above. Nine-week-old *Rag-2^{-/-} γ c^{-/-}* mice (Taconic, Germantown, NY) were irradiated with 7 Gy and engrafted with 400 000 Lin⁻ BM cells from donor mice by tail vein injection.²³ Seven and 25 weeks after injection of the cells, peripheral blood obtained from the retro-orbital sinus was analyzed by flow cytometry. Donor-derived T and B cells were detected using anti-CD4-biotin (streptavidin-FITC), anti-CD8 α -PE-Cy7, and anti-B220-PE-Cy5 antibodies. T and B cells of *Rag-2^{-/-} γ c^{-/-}* mice reconstituted with control or *PtcH* mutant Lin⁻ BM cells were isolated using magnetic-activated cell sorting (MACS) separation columns (Miltenyi Biotec, Auburn, CA), and *ERT2*-mediated recombination of *PtcH* alleles was analyzed as described.

Results

Postnatal inactivation of *PtcH* alleles

Proper genomic recombination of the *PtcH^{lox}* targeting vector (*pPtcH^{lox}*) into the wt *PtcH* allele in R1 embryonic stem cells was analyzed by Southern blot hybridization and by PCR from genomic DNA (Figure 1B and 1C, respectively). Positive embryonic stem-cell clones were injected into blastocysts of C57BL/6 mice, and resulting chimeras were bred to wt C57BL/6 females. Heterozygous *PtcH^{lox/+}* offspring were intercrossed to obtain the homozygous *PtcH^{lox/lox}* mouse line. *PtcH^{lox/lox}* mice were born at the expected Mendelian ratio. All heterozygous and homozygous mice remained healthy over an observation period

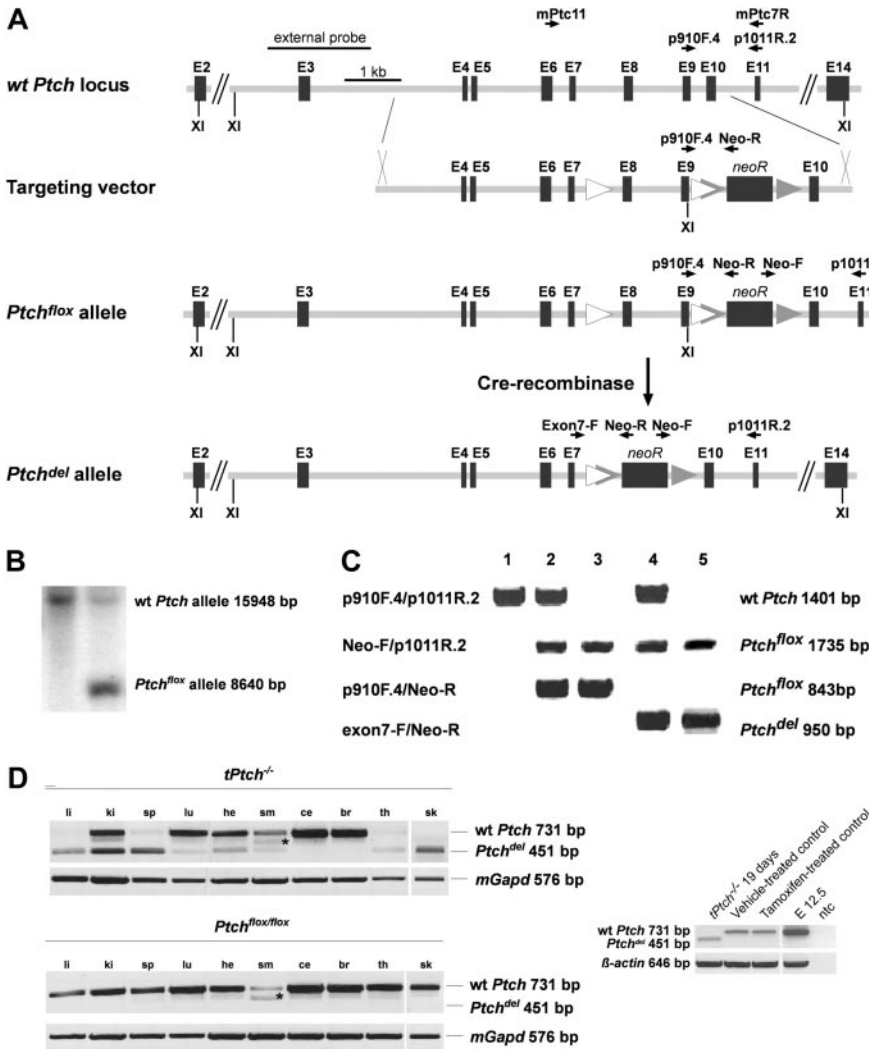


Figure 1. CreERT2-mediated inactivation of *Ptch*. (A) Part of the wild-type (wt) murine *Ptch* allele and the targeting vector, which upon homologous recombination generates *Ptch^{flox}* that harbors *loxP* sites (Δ) 5' and 3' of exons 8 and 9 as well as a *frt*-flanked (Δ) neomycin resistance cassette in intron 9. Following tamoxifen treatment, Cre-mediated recombination generates the inactivated *Ptch^{del}* allele. The external probe used for Southern blot analysis of ES-cell transfectants and primers used for mouse genotyping and amplification of transcripts are indicated (see "Materials and methods" for details). XI indicates *XhoI*. (B) Using the external probe, Southern blot analysis of *XhoI*-digested DNA distinguishes wt *Ptch* and *Ptch^{flox}*, which give rise to a 15 948- and 8640-bp fragment, respectively. (C) Primer pairs indicated on the left and depicted in panel A identify genomic wild-type *Ptch*, *Ptch^{flox}*, and *Ptch^{del}* alleles by PCR performed on either mouse tail DNA (lanes 1-3) or DNA preparations from mouse embryos (lanes 4-5). The 1735-bp fragment amplified by the primer pair Neo-F/p1011R.2 identifies all floxed *Ptch* alleles. Loss of the 843-bp fragment amplified with primers p910F.4/Neo-R demonstrates successful Cre-mediated recombination. (Lane 1) Homozygous wild-type *Ptch* alleles, (lane 2) heterozygous *Ptch^{flox/+}* alleles, (lane 3) homozygous *Ptch^{flox/flox}* alleles, (lane 4) heterozygous *Ptch^{del/+}*, and (lane 5) homozygous *Ptch^{del/del}* alleles. (D) Recombination efficiencies in *tPtch^{-/-}* mice (top panel) and vehicle-treated *Ptch^{flox/flox}ERT2^{-/-}* mice (middle panel) from the indicated organs were analyzed on cDNA-level using primer pair mPtc11/mPtc7R (for location, see panel A). Recombination efficiency in bone marrow (BM) is shown separately (bottom panel). The amplification of a 451-bp fragment indicates transcripts of the *Ptch^{del}* allele. The fragment marked by an asterisk results from a normal *Ptch* splice variant, in which exon 10 is missing.²⁴ Amplification of *mGapd* or *β-actin* served as control. cDNA obtained from day-12.5-old embryos (E12.5) served as positive control. li indicates liver; ki, kidney; sp, spleen; lu, lung; he, heart; sm, skeletal muscle; ce, cerebellum; br, brain; th, thymus; sk, skin; and ntc, no template control.

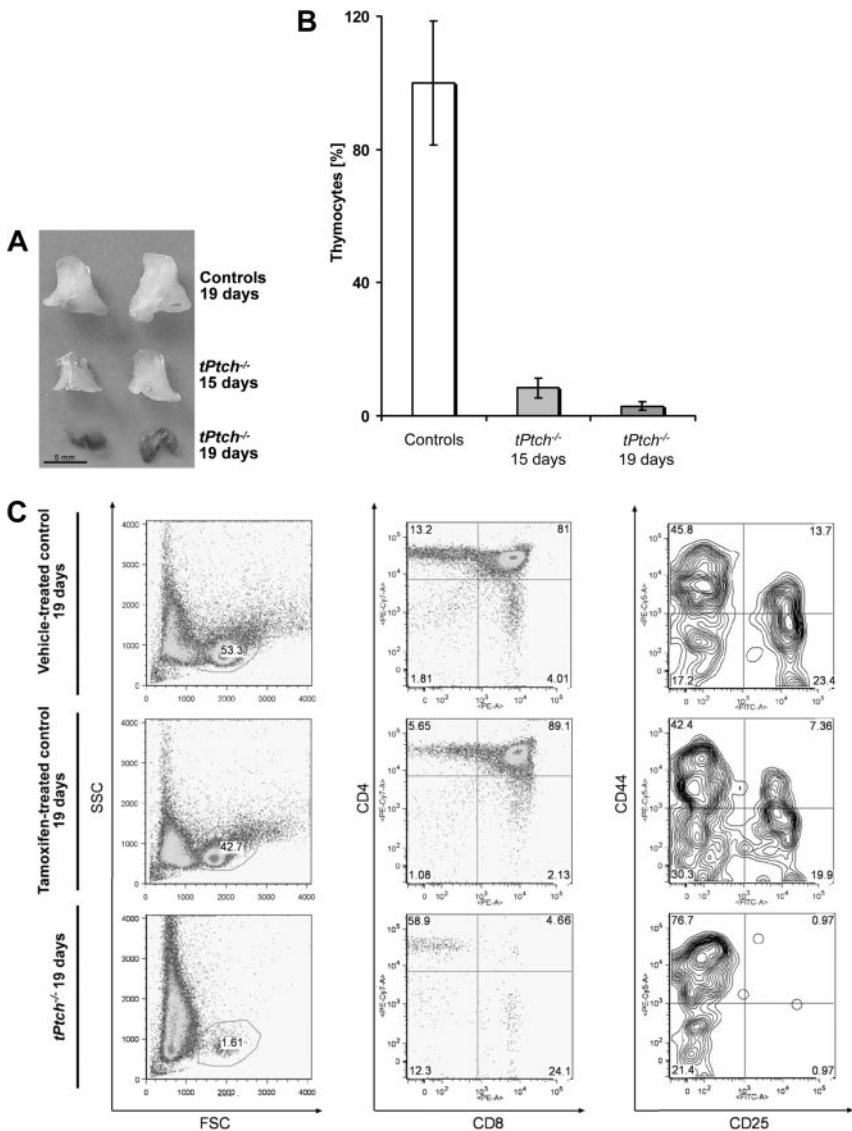
of 15 months and were phenotypically normal and fertile. Neither the *loxP* sides in intron 7 nor the neomycin resistance cassette in intron 9 disturbed the normal splicing of the *Ptch* mRNA derived from the *Ptch^{flox}* allele. The cDNA amplification using the primer combination mPtc11/mPtc7R (Figure 1A) did not reveal any abnormal splicing variants from the *Ptch^{flox}* allele in *Ptch^{flox/+}* and *Ptch^{flox/flox}* mice compared with wild-type (wt) mice (Figure 1D). Postnatal inactivation of *Ptch* was analyzed in *Ptch^{flox/flox}ERT2^{-/-}* mice by application of tamoxifen to induce Cre recombinase activity. The recombination efficiency of Cre-mediated deletion of exons 8 and 9 of the *Ptch^{flox}* alleles (*Ptch^{del}* allele) was demonstrated by quantitative PCR of genomic DNA. Ten days after the first tamoxifen injection, the deletion efficiency was nearly 100% in BM of *Ptch^{flox/flox}ERT2^{-/-}* (hereafter *tPtch^{-/-}*) mice. Since both nonstromal and stromal cells contribute to whole BM, *Ptch* must have been deleted in both cell compartments. More than 75% *Ptch^{flox}* alleles in liver, kidney, spleen, thymus, and skin from *tPtch^{-/-}* mice were converted into *Ptch^{del}* alleles. The recombination efficiency in lung, heart, and skeletal muscle was more than 50%, whereas in cerebellum and brain less than 25% of the *Ptch^{flox}* alleles were converted into *Ptch^{del}* alleles (data not shown). These results were confirmed by reverse-transcription (RT)-PCR and revealed expression of mutant *Ptch^{del}* transcripts in the analyzed tissues (Figure 1D). Thus, tissue specificity and recombinase efficiency

of Cre in *ERT2* mice appear to be identical to those reported for Mx1Cre mice, which are frequently used for immunologic studies.²⁵

Thymic atrophy and defective T-cell development in *tPtch^{-/-}* mice

Fifteen days after the first tamoxifen injection, *tPtch^{-/-}* thymi were markedly smaller and the total number of thymocytes was 13-fold decreased compared with control animals (Figure 2A,B). At day 19, the thymus of *tPtch^{-/-}* mice had lost its regular morphology and the cortex was no longer distinguishable from the medulla (Figure 2A and data not shown). Only a few thymocytes were left at this stage (Figure 2B,C left panel). Although a moderate reduction of thymocyte numbers was also observed in tamoxifen-treated *Ptch^{flox/flox}ERT2^{-/-}* control animals (Figure 2C left and middle panels), our data indicated a role of Ptch on thymocyte differentiation, which is consistent with previous reports.⁷ We thus monitored distinct T-cell populations by flow cytometry. Although the absolute numbers of all subpopulations were lowered in *tPtch^{-/-}* mice (data not shown), the relative numbers of immature double-negative (DN, CD4⁻CD8⁻) and mature single-positive (CD4⁺ or CD8⁺) T cells were strongly increased, whereas the double-positive (DP, CD4⁺CD8⁺) population was almost depleted in *tPtch^{-/-}* thymi 19 days after tamoxifen injection (Figure 2C middle panel). This result

Figure 2. Thymus atrophy and loss of thymocytes in *tPtch*^{-/-} mice. (A) Thymi from vehicle-treated control animals (top row) and thymus from *tPtch*^{-/-} mice 15 and 19 days after the first tamoxifen injection (middle and bottom rows, respectively). (B) Fifteen and 19 days after tamoxifen injection, thymocyte numbers of *tPtch*^{-/-} mice were determined by flow cytometry SSC versus FSC plot (n = 4 and n = 3, respectively) and are expressed as relative numbers compared with those obtained from control animals (n = 9 for tamoxifen- and n = 7 for vehicle-treated animals of both time points). Error bars represent standard deviation of the mean. (C) Thymocytes of *tPtch*^{-/-} mice were prepared 19 days after the onset of tamoxifen treatment and analyzed by flow cytometry. Cells from vehicle-treated *Ptch*^{fllox/fllox}*ERT2*^{+/-} and tamoxifen-treated *Ptch*^{fllox/fllox}*ERT2*^{-/-} animals served as controls. Thymocytes within the lymphocyte fraction (SSC versus FSC, left panels) were analyzed by anti-CD4/anti-CD8 and anti-CD44/anti-CD25 stainings (middle and right panels, respectively). Relative percentages of the different thymocyte populations are indicated. Data are representative of 4 independent experiments (each experiment consisted of 1 vehicle-treated *Ptch*^{fllox/fllox}*ERT2*^{+/-}, 1 tamoxifen-treated *Ptch*^{fllox/fllox}*ERT2*^{-/-}, and 1 *tPtch*^{-/-} mouse).



suggested that DN T-cell precursors require thymic PtcH expression to progress to the DP stage.

Four early stages of DN-cell differentiation can be discriminated based on the expression of CD25 and CD44 surface markers. The DN1 population (CD25⁻CD44⁺) possesses multilineage potential, while DN2 (CD25⁺CD44⁺) and DN3 (CD25⁺CD44⁻) cells commit to the T-cell lineage before they further develop into DN4 cells (CD25⁻CD44⁻).²⁶ In *tPtch*^{-/-} thymi, the DN1 population was considerably overrepresented, whereas DN2 and DN3 populations were diminished (Figure 2C right panel). The relative number of DN4 cells remained stable within the entire observation period. Collectively, our data show that upon *Ptch* ablation early thymocyte development is blocked at 2 stages (ie, at the transitions from DN1 to DN2 and DN4 to DP).

PtcH ablation compromises splenic B-cell development

We next assessed a possible role of *Ptch* ablation on peripheral B-cell subsets. Splenic B220-positive B lymphocytes can be distinguished based on their expression patterns of CD21, CD24, and the B-cell antigen receptor (BCR) of classes IgM and IgD.²⁷ Transitional B cells of type 1 (T1, CD24⁺CD21⁻IgM^{high}IgD^{low}) are

recent immigrants from the BM and develop into transitional type 2 B cells (T2, CD24⁺CD21⁺IgM^{high}IgD^{high}). Mature B lymphocytes (CD24^{low}CD21^{low}IgM^{low}IgD^{high}) can be generated from both T1 and T2 B cells.²⁷ In *tPtch*^{-/-} spleens, the absolute number of B220-positive cells was reduced compared with the respective controls (data not shown). This was due mainly to a reduction of the population of T1 B cells. This is also reflected by their relative numbers that are drastically diminished compared with vehicle- and tamoxifen-treated control animals (Figure 3). In contrast, the pool of the more mature T2 cells remained stable and mature B cells were overrepresented. This effect was detected already at day 15 after treatment onset (data not shown) and progressed until day 19. Thus, in the spleen of *tPtch*^{-/-} mice, the supply of immature B cells from the BM is severely impaired suggesting a role of PtcH on early B-cell differentiation.

PtcH is required for B-cell differentiation in the BM

B-cell lymphopoiesis in the BM can be monitored by cell-surface staining of B220, CD43, and IgM. B220 and CD43 are both expressed on early B-cell precursors prior to the pro-B-cell stage, which is defined as B220^{low}CD43⁺IgM⁻. Progression to the pre-B-cell stage is associated with loss of CD43 and

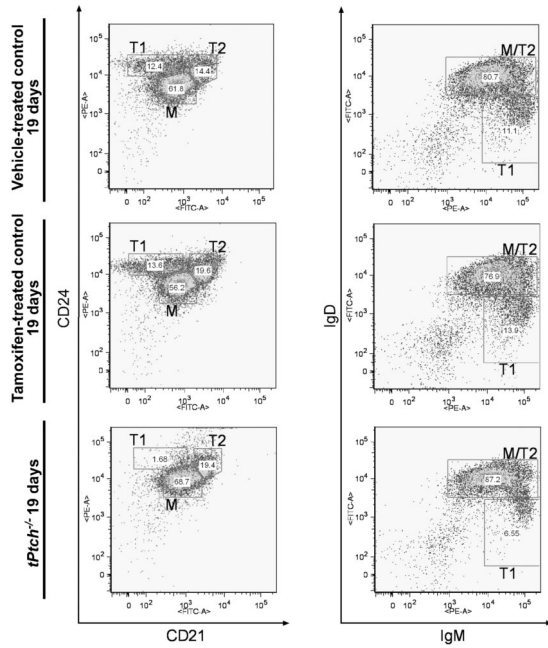


Figure 3. Splenic T1 B cells are lost in *tPtch*^{-/-} mice. Splenocytes of vehicle-treated *Ptch*^{fllox/fllox}*ERT2*^{+/-} or tamoxifen-treated *Ptch*^{fllox/fllox}*ERT2*^{-/-} controls and of day-19 *tPtch*^{-/-} mice were analyzed by flow cytometry using antibodies against B220, CD21, CD24, IgM, and IgD to distinguish T1, T2, and mature (M) B cells. (Left panels) Within the B220-positive fraction, T1 cells are CD24⁺CD21⁻, T2 are CD24⁺CD21⁺, and mature B cells are CD24^{low}CD21^{low}. (Right panels) Within the B220-positive fraction, T1 cells are IgM^{high}IgD^{low}, T2 cells are IgM^{high}IgD^{high}, and mature B cells are IgM^{low}IgD^{high}/B220⁺. The number of cells present in each fraction is presented as relative percentage of the total cell number plotted. Data are representative of 4 independent experiments (each experiment consisted of 1 vehicle-treated *Ptch*^{fllox/fllox}*ERT2*^{+/-}, 1 tamoxifen-treated *Ptch*^{fllox/fllox}*ERT2*^{-/-}, and 1 *tPtch*^{-/-} mouse).

expression of the pre-BCR encompassing the μ m heavy chain (B220⁺CD43^{low} μ m⁺). B220 expression increases on immature B cells (B220^{high}CD43⁻IgM^{low-high}) and is maintained on immunocompetent recirculating B cells, which additionally express the IgD-BCR (B220^{high}CD43⁻IgM^{low}IgD^{high}).²⁸ The total lymphocyte fraction in the BM of *tPtch*^{-/-} mice was only slightly

decreased compared with wt controls (Figure 4 left panel). Striking alterations were, however, observed for the individual BM B-cell subsets in *tPtch*^{-/-} mice. Cell-surface staining of B220 versus CD43 revealed an almost complete loss of CD43⁺ progenitor B cells (Figure 4 middle panel, fraction II), which in turn led to a dramatic loss of B220^{low} pre-B and immature B cells (right panel, fractions I and II). Conversely, the relative numbers of recirculating B lymphocytes, which are B220^{high} (Figure 4 middle and right panel, fraction III) and IgD positive (data not shown), were strongly increased. A similar distribution of BM B-cell subsets was observed when counting the absolute cell numbers (data not shown). A moderate effect of tamoxifen on the pro-, pre-, and immature B cells was observed at day 15 in all tamoxifen-treated control mice (data not shown); this effect was almost compensated at day 19 of treatment (Figures 3,4). Collectively, our data reveal a severe block of early B-cell development in *tPtch*^{-/-} mice prior to the pro-B-cell stage.

Lineage specification of CLPs is defective in *tPtch*^{-/-} mice

Since *Ptch* ablation affected both T- and B-cell lineages, we next analyzed their common precursors in our mutant mice. Within the pool of lineage-negative (Lin⁻) cells in the BM, those with small and nongranule appearance harbor both HSCs and more committed descendant precursors.²⁹ HSCs normally express high levels of c-kit and Sca-1, which are down-regulated in committed progenitors.³⁰ As shown in Figure 5A (left panel), the HSC-containing Lin⁻c-kit^{high}Sca-1^{high} cell population III was relatively increased in *tPtch*^{-/-} mice as was the fraction I of Lin⁻c-kit^{high}Sca-1^{low} cells, which comprises most of the myeloid progenitors.^{28,31,32} In marked contrast, the CLP-containing fraction II (Lin⁻c-kit^{low}Sca-1^{low})²⁶ was underrepresented and its relative cell number was reduced by half. Hence *Ptch* ablation appears to compromise CLPs. This notion was further confirmed by expression analysis of IL-7R α chain (Figure 5A right panel), which is required for the generation of CLPs. In *tPtch*^{-/-} mice, the number of IL-7R α -expressing cells within the CLP-containing fraction II (Lin⁻c-kit^{low}Sca-1^{low}) was drastically reduced compared with controls. Moreover, BrdU/7-AAD stainings shown in Figure 5B revealed a markedly reduced

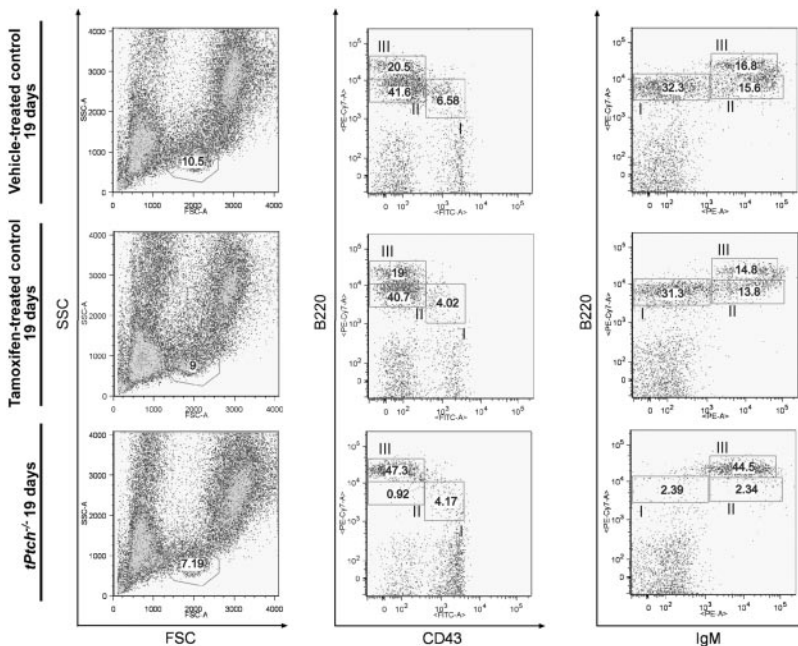


Figure 4. Early block of B-lineage commitment in the BM of *tPtch*^{-/-} mice. BM cells from vehicle- and tamoxifen-treated control animals and of day-19 *tPtch*^{-/-} mice were analyzed by flow cytometry using antibodies against B220, CD43, and IgM (middle and right panels) to distinguish pro-B (fraction I), pre-B (fraction II), and the pool encompassing immature, mature, and recirculating B cells (fraction III) within the lymphocyte gate defined by the SSC/FSC plots (left panels). Data represent 4 independent experiments (each experiment consisted of 1 vehicle-treated *Ptch*^{fllox/fllox}*ERT2*^{+/-}, 1 tamoxifen-treated *Ptch*^{fllox/fllox}*ERT2*^{-/-}, and 1 *tPtch*^{-/-} mouse).

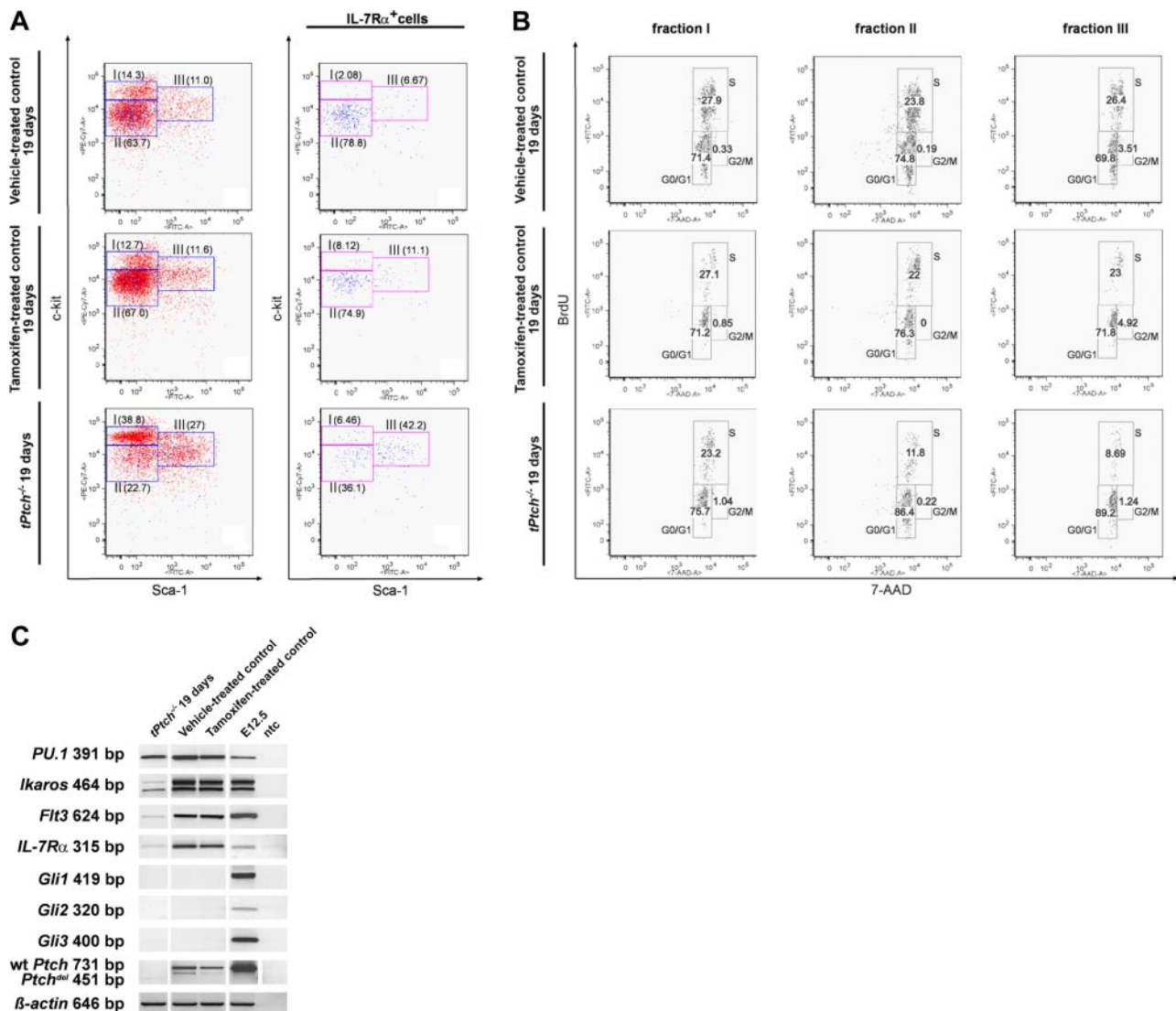


Figure 5. Early B-cell development is compromised at the CLP stage in *tPtch*^{-/-} mice. (A) Lin⁻ BM cells from vehicle- and tamoxifen-treated control animals and of day-19 *tPtch*^{-/-} mice were analyzed by flow cytometry using antibodies against c-kit and Sca-1 (left panels). Fraction I (Lin⁻c-kit^{high}Sca-1^{low}) contains mainly precursors of the myeloid lineages, fraction II (Lin⁻c-kit^{low}Sca-1^{low}) represents the CLP-containing compartment, and fraction III (Lin⁻c-kit^{high}Sca-1^{high}) contains uncommitted HSCs and MPPs. The IL-7Rα⁺ cells within these fractions are shown in the right panels. Data are representative of 3 independent experiments (each experiment consisted of 1 vehicle-treated *Ptch*^{fllox/fllox}*ERT2*^{-/-}, 1 tamoxifen-treated *Ptch*^{fllox/fllox}*ERT2*^{-/-}, and 1 *tPtch*^{-/-} mouse). (B) Three hours after intraperitoneal injection of BrdU, Lin⁻ cells of control and day-19 *tPtch*^{-/-} mice were isolated and labeled with 7-amino actinomycin D (7-AAD), and cells in fractions I to III (described in A) were analyzed by flow cytometry. Data are representative of 3 independent experiments (each experiment consisted of 1 vehicle-treated *Ptch*^{fllox/fllox}*ERT2*^{-/-}, 1 tamoxifen-treated *Ptch*^{fllox/fllox}*ERT2*^{-/-}, and 1 *tPtch*^{-/-} mouse). (C) Lin⁻ BM cells of vehicle- and tamoxifen-treated control animals and of day-19 *tPtch*^{-/-} mice were isolated, and RT-PCR analysis was performed to monitor expression of the genes indicated on the left. cDNA obtained from day-12.5-old embryos (E12.5) served as positive control. ntc indicates no template control. White vertical lines have been inserted to indicate where a gel lane was cut. All lanes within each individual row are from one and the same experiment.

proliferative capacity of cells in fraction II from *tPtch*^{-/-} mice (middle panel). This was also true for cells in fraction III (Lin⁻c-kit^{high}Sca-1^{high}), which contains HSCs and MPPs (right panel). Importantly, myeloid precursors of fraction I (Lin⁻c-kit^{high}Sca-1^{low}) proliferated normally (left panel).

Final evidence for a CLP deficiency in *tPtch*^{-/-} mice was obtained by expression analysis of key transcription factors. The Ets-related transcription factor PU.1 is expressed in all Lin⁻ cells and supports maintenance of HSCs.³³ Transcription of *PU.1* in Lin⁻ cells of *tPtch*^{-/-} mice was unaltered (Figure 5C), suggesting that the earliest stages of hematopoiesis do not require Ptch. In contrast, transcription of *Ikaros*, *Flt3*, and *IL-7Rα*, 3 marker genes known to be important for specification of CLP and also myeloid lineages,³⁴ was hardly detectable, which is consistent with a loss of CLP upon Ptch ablation. The complete absence of transcripts for

EBF and Rag-1/2 in Lin⁻ BM cells of *tPtch*^{-/-} mice demonstrated the inability of the progenitor cells to recombine antigen receptor genes and to initiate lymphocyte differentiation. In summary, our results reveal a *Ptch* mutation-induced specification defect of the lymphoid lineage at the level of CLPs in the BM. However, we found no induction of *Gli* transcription in Lin⁻ BM cells of *tPtch*^{-/-} mice (Figure 5C), which is usually associated with loss of Ptch-mediated Smo inhibition.^{12,35} It thus appears that upon tamoxifen treatment, Ptch-negative cells are rapidly lost from the BM.

Specification defect of the lymphoid lineage depends on Ptch function in the stromal cell compartment

So far our data established a mandatory role of Ptch for CLP formation. Targeted *Ptch* disruption in our mice is, however, not

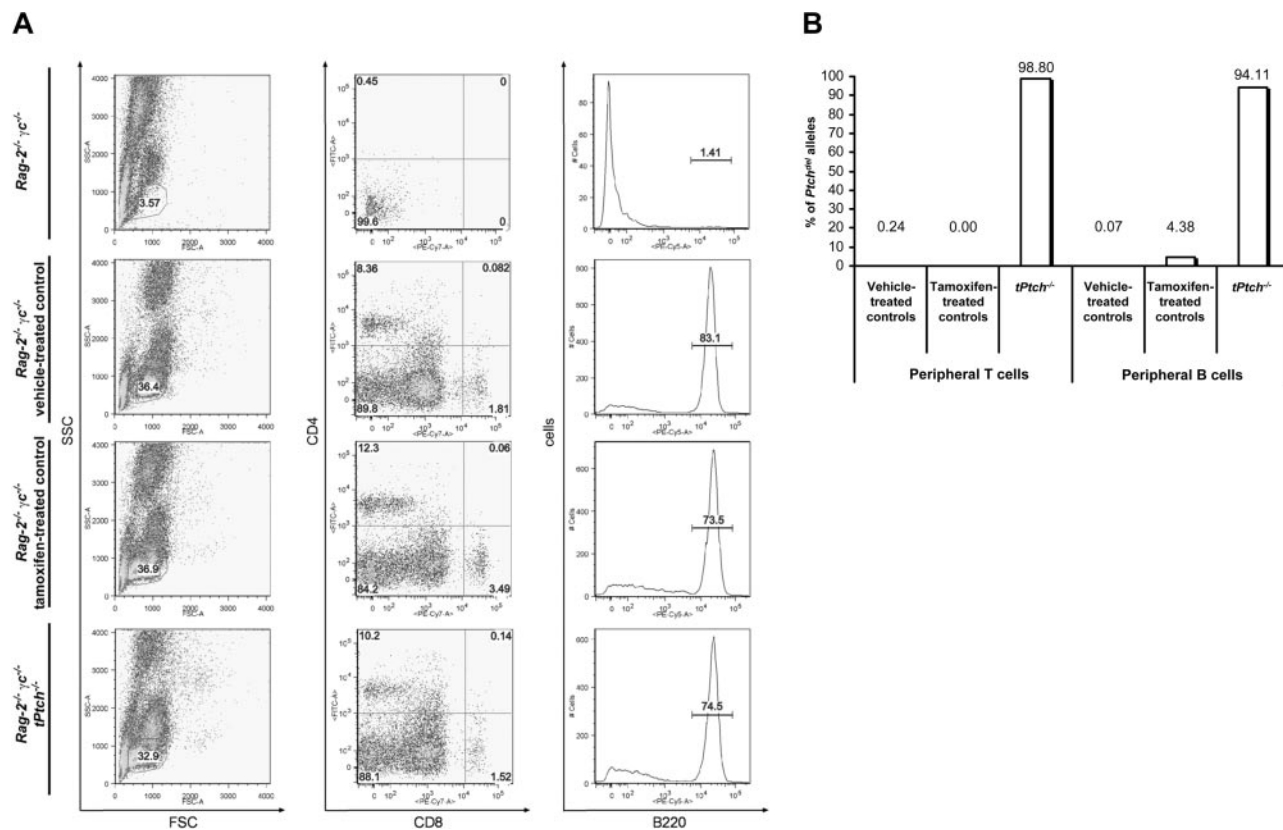


Figure 6. Specification defect of the lymphoid lineage in *tPtch*^{-/-} mice is dependent on stromal BM cells. Lin⁻ BM cells (400 000) from vehicle- and tamoxifen-treated control animals or day-19 *tPtch*^{-/-} mice were injected intravenously into lethally irradiated *Rag-2*^{-/-} γ *c*^{-/-} mice. After 7 weeks, peripheral blood cells were analyzed by flow cytometry (A). Cells within the lymphocyte gate (left panels) were analyzed by staining with antibodies against either CD4 and CD8 (middle panel) or B220 to identify T and B cells, respectively. Nonreconstituted *Rag-2*^{-/-} γ *c*^{-/-} mice served as negative control (top row). The presence of inactivated *Ptch* alleles in T and B cells from reconstituted *Rag-2*^{-/-} γ *c*^{-/-} mice was detected by quantitative PCR (B). Data are representative of 3 independent experiments (each experiment consisted of the transfer of Lin⁻ BM cells derived from 1 vehicle-treated *Ptch*^{fllox/lox}E^{RT2}^{+/+}, 1 tamoxifen-treated *Ptch*^{fllox/lox}E^{RT2}^{-/-}, and 1 *tPtch*^{-/-} mouse).

cell-type specific and hence we cannot discriminate between cell-autonomous and heterologous (ie, stromal cell-dependent) defects. To distinguish between these possibilities, Lin⁻ BM cells were purified from *tPtch*^{-/-} mice and adoptively transferred into irradiated *Rag-2*^{-/-} γ *c*^{-/-} mice, which lack T and B cells³⁶ and that express *Ptch* in the residual thymus as well as in BM stromal cells (data not shown). Lin⁻ BM grafts from vehicle- or tamoxifen-treated mice served as controls. As shown in Figure 6A, repopulation of peripheral blood lymphocytes was achieved in all cases and with the same efficiency (left panel). The Lin⁻ BM cells from *Ptch* mutant mice reconstituted mature CD4⁺ and CD8⁺ single-positive T cells (middle panel) as well as B220-positive B cells (right panel) and with the same frequency than wt BM cells did. Importantly, quantitative PCR analysis showed that 99% of *Ptch*^{fllox} alleles in the transferred BM cells were inactivated by recombination (Figure 6B), which is consistent with the observation that almost all T and B cells derived from *tPtch*^{-/-} mice were deficient for *Ptch* expression (data not shown). Similar results were obtained by assessment of T and B cells after long-term population (25 weeks), in adoptive transfer experiments with severe combined immunodeficient (SCID)/beige mice or when *Ptch* was deleted after establishment of chimerism in *Rag-2*^{-/-} γ *c*^{-/-} mice (data not shown). Since the *Ptch* homologue *Ptch2* is not expressed in T and B cells (data not shown), it does not functionally substitute *Ptch*. These experiments show that *Ptch* function, itself, in CLPs appears to be dispensable for proper progression along the T- and B-cell lineages. Rather, *Ptch* function by the inductive environment, most likely stromal cells, is required for CLP differentiation.

Normal specification of the granulocyte-macrophage lineage in *tPtch*^{-/-} mice

So far we had no indication for myeloid deficiencies in *tPtch*^{-/-} mice. To analyze this aspect in more detail, we investigated the myeloerythroid colony-forming activity within the Lin⁻ fraction of the *tPtch*^{-/-} BM 19 days after the first tamoxifen injection. We found no effect of *Ptch* disruption on the differentiation of the multipotent CFU-granulocyte/erythrocyte/megakaryocyte/macrophage (CFU-GEMM), bi- or unipotential CFU-granulocyte/macrophage (CFU-GM), CFU-granulocyte (CFU-G), CFU-macrophage (CFU-M) and burst-forming unit-erythroid (BFU-E) progenitors (Table 1). Efficient *Ptch* ablation in CFU-GEMM colonies derived from *tPtch*^{-/-} mice was demonstrated by PCR (data not shown). We also investigated the morphology and distribution of all peripheral blood cells by automated blood cell counts, blood smear tests, and FACS analysis (Tables 2,3). Consistent with the specification defect of the lymphoid lineage, we found a reduction of peripheral lymphocytes in *tPtch*^{-/-} mice compared with control animals. Except for an increase in the number of neutrophilic granulocytes, the number and morphology of all other blood cells remained normal. The high number of neutrophils in *tPtch*^{-/-} mice is most likely a secondary effect of the *Ptch* ablation as this is associated with skin lesions and tumor formation (data not shown). However, these data show that *Ptch* is dispensable for development and specification of myeloid lineages.

Table 1. Cell counts of BM and of peripheral blood samples and clonogenic progenitor assay of Lin⁻ BM cells from control and *tPtch*^{-/-} mice

	Controls			<i>tPtch</i> ^{-/-} (19 days)			<i>P</i>
	Mean	Deviation	n	Mean	Deviation	n	
CFU-GEMM	0.6	0.8	5	0.5	0.5	4	.811
CFU-GM	16.9	6.4	5	13.9	6.8	4	.312
CFU-G	45.8	6.0	5	48.5	12.2	4	.394
CFU-M	62.8	5.7	5	61.7	15.7	4	.635
BFU-E	2.8	1.8	5	2.3	1.4	4	.534

Progenitor activity of Lin⁻ BM cells from *tPtch*^{-/-} mice and from respective controls was examined 19 days after the onset of tamoxifen treatment using the colony-forming assay. Lin⁻ BM cells (2×10^3) were cultured in methylcellulose-containing medium on a 35-mm dish. Lin⁻ BM cells of each animal were tested in triplicates. Numbers of colonies/dish were counted after 8 days. Data for controls were pooled from both vehicle- and tamoxifen-treated animals.

n indicates the number of tested animals.

Discussion

With this paper, we have established a nonredundant inducer function of PtcH for the specification of B- and T-cell lineages. Targeted disruption of *PtcH* in the adult mouse severely compromises the CLP-containing cell population in the BM resulting in a depletion of early B-cell descendants in the spleen and abrogated differentiation of intrathymic T-cell progenitors. The CLP differentiation deficit is not cell autonomous as PtcH-negative BM cells are capable of fully reconstituting functional B- and T-cell compartments in *Rag-2*^{-/-}*γc*^{-/-} mice. We conclude that the generation and/or maintenance of CLPs requires PtcH expression by the stromal-cell compartment. In contrast, myeloid lineage commitment is PtcH independent.

Several lines of evidence show that the specification defect of the entire lymphoid lineage in *PtcH* mutant mice occurs at the level of CLPs or even earlier in the BM. First, the number of IL-7Rα-expressing cells within the Lin⁻c-kit^{low}Sca-1^{low} fraction, which represents CLPs,^{1,37} is reduced in *tPtch*^{-/-} mice. Second, the proliferative capacity of the CLP-containing fraction and also that of their immediate progenitors, which are maintained in the Lin⁻c-kit^{high}Sca-1^{high} fraction,³⁸ is reduced. Third, expression of

Table 2. Hematologic parameters of *tPtch*^{-/-} and control mice 19 days after the onset of tamoxifen treatment

	Controls			<i>tPtch</i> ^{-/-} (19 days)			<i>P</i>
	Mean	Deviation	n	Mean	Deviation	n	
Hkt	0.425	0.028	7	0.409	0.062	5	.663
Hgb, g/dL	134.0	6.0	6	131.0	18.0	5	.810
Ery, $\times 10^9/L$	9.4	1.6	7	8.0	1.2	5	.307
Re	40.5	19.6	10	33.8	5.6	4	.267
Leu, $\times 10^9/L$	0.0061	0.0019	7	0.0077	0.0038	5	.518
Pl, $10^9/L$	28.70	18.77	6	31.96	14.75	5	.807
Ne	0.257*	0.091*	11	0.474*	0.171*	7	.011*
Ly	0.655*	0.083*	11	0.390*	0.091*	8	.001*
Mo	0.041	0.032	11	0.030	0.019	8	.521
Eo	0.020	0.019	11	0.040	0.041	7	.341
Ba	0.028	0.024	11	0.059	0.045	7	.143

Blood cell numbers were determined both by an automated hematological analyzer or by analyzing blood smears. Hkt, Ne, Ly, Mo, Eo, and Ba are given as proportions of 1.0. Re are given as the proportion of 1000 Ery.

Hkt indicates hematocrit; Hgb, hemoglobin; Ery, erythrocytes; Re, reticulocytes; Leu, leukocytes; Pl, platelets; Ne, neutrophil granulocytes; Ly, lymphocytes; Mo, monocytes; Eo, eosinophil granulocytes; and Ba, basophil granulocytes.

*Significant differences (*P* value < .05 by Mann-Whitney *U* test) between *tPtch*^{-/-} and control mice.

Table 3. Numbers of peripheral T and B cells of *tPtch*^{-/-} and control mice 19 days after onset of tamoxifen treatment

	Controls			<i>tPtch</i> ^{-/-} (19 days)			<i>P</i>
	Mean	Deviation	n	Mean	Deviation	n	
Ly, % FACS	46.70*	11.63*	7	23.34*	9.53*	5	.012*
B cells, %	13.98*	3.74*	7	4.71*	2.33*	5	.004*
CD4 ⁺ T cells, %	6.94	3.50	7	4.83	1.36	5	.333
CD8 ⁺ T cells, %	2.90	1.61	7	2.17	1.06	5	.454

Cell numbers were determined by FACS analyses from the lymphocyte gate using anti-B220 (B cells), and anti-CD4 and anti-CD8 (T cells) antibodies.

Ly indicates lymphocytes.

*Significant differences (*P* value < .05 by Mann-Whitney *U* test) between *tPtch*^{-/-} and control mice.

Ikaros and the cell-surface receptor *Flt3*, which are expressed on lymphoid-primed multipotent progenitors,³⁴ was partially down-regulated in Lin⁻ BM cells of *tPtch*^{-/-} mice. The absence of Rag-1 and Rag-2 expression prevents the initiation antigen receptor gene recombination and explains the failure of B-cell progenitors to enter the pre-B-cell stage. In *tPtch*^{-/-} thymi, T-cell progenitors do not differentiate beyond the DN1 stage, which explains the involution of the cortical thymus region, where differentiation into DN2 and DN3 normally occurs.³⁹ Consistent with our data, Shah et al demonstrated that Hh plays an important role for the expansion of DN1 cells and their transition into DN2.⁹ While Hh has been shown to arrest thymocyte development at the DN3 stage in vitro,⁹ PtcH apparently does not play a major role in this process but appears to be required for the transition of DN4 to DP, because the pool of DN4 T cells is maintained in *tPtch*^{-/-} thymi 19 days after PtcH inactivation. Thymic atrophy and reductions of the immature DN and DP compartments associated with a relative increase of mature single-positive thymocytes have been also achieved by a Mx1Cre-mediated deletion of Smo, the downstream signaling partner of PtcH.⁷

In contrast to CLPs, the differentiation potential of the HSC- and MPP-containing Lin⁻c-kit^{high}Sca-1^{high} population appears to be normal, although we observed a slightly decreased proliferative capacity of these cells. These results are in agreement with data showing that Hh treatment of cord blood HSCs affects their proliferative capacity, but has no effect on cell fate.⁵ In *tPtch*^{-/-} mice, the Lin⁻c-kit^{high}Sca-1^{low} fraction, which contains CMPs and the downstream GMPs and MEPs,² proliferated normally. Moreover, the numbers of CFU progenitors as well as the majority of the corresponding peripheral blood cells in *tPtch*^{-/-} animals were indistinguishable from those of control animals. The number of thrombocytes was unchanged in the mutants, which demonstrates continuous thrombocyte generation from HSCs and is indicative of normal HSC function.^{2,26} The elevated numbers of blood neutrophils in *tPtch*^{-/-} mice are probably caused by inflammatory processes due to precancerous lesions in several organs including stomach and skin (data not shown). The poor general condition of the mutant animals prevented us from investigations beyond day 21 of tamoxifen treatment onset. However, the morphology of all peripheral blood cells remained normal and we did not observe leukemogenesis within the observation period of 19 days. Collectively, our experiments demonstrate that PtcH deficiency targets the branching point of MPP differentiation into CLPs and CMPs. While CLP formation and/or maintenance require PtcH, CMP generation and function do not.

The successful repopulation of peripheral B and T cells from PtcH-negative BM cells in irradiated *Rag-2*^{-/-}*γc*^{-/-} mice shows that PtcH expression, itself, in CLPs is dispensable for proper lymphoid lineage commitment. Rather, the result strongly suggests a critical role of PtcH for the functionality of the inductive

environment (ie, the stromal-cell compartment) that is necessary for lymphoid versus myeloid differentiation. One example of such a binary cell fate determinant on stromal cells is provided by the Jagged/Delta-like protein, which is the ligand for Notch expressed on thymocytes and directs T- versus B-cell development (for review see Germain⁴⁰). However, we cannot formally exclude a cell-autonomous function of Ptch in developing T cells, which would be consistent with the reported expression of Ptch during all DN stages.⁷ The fate of Ptch-deficient BM cells, the Hh/Ptch effector mechanisms, and how exactly they regulate lymphoid lineage commitment remain to be elucidated in future studies.

Acknowledgments

This work was supported by a grant of the Wilhelm Sander Stiftung no. 2003.112.1 to H.H. K.D. and J.W. were supported by the Deutsche Forschungsgemeinschaft through FOR 521.

We are grateful to Alexandra Pahl, Kerstin Beyer, and Stefan Wolf for excellent animal care; Ina Hess, Astrid Herwig, Gabi Hindermann, and Martha Zientkowska for technical assistance; and Michael Engelke for technical advice. We thank Marcus Conrad (Institute of Clinical Molecular Biology and Tumor Genetics, GSF, Munich) for providing the cloning vector pPNT4; Wolfgang Wurst (Institute of Developmental Genetics, GSF, Munich) for advice; Hermann Riedesel (MPI for Experimental Medicine, Goettingen) for the support in breeding knock-out mice; Anton Berns and Ate Loonstra (The Netherlands Cancer Institute, Amsterdam, The Netherlands) for provid-

ing *Rosa26CreERT2* mice; and Leszek Wojnowski (University of Mainz) for comments on the paper.

Authorship

Contribution: A.U. and K.D. designed and performed research, collected and analyzed data, and wrote the paper; F.N. designed and performed the research, and collected and analyzed data; R.D. designed and performed research; M.K. designed and performed the research, and collected and analyzed data; A.F. performed the research and collected data; A.Z. designed and performed research, and collected and analyzed data; C.B. designed and performed research, and collected and analyzed data; I.A. designed and performed the research; M.N. designed and performed research; T.H. performed research and collected data; V.A. designed research; W.S.-S. designed research, contributed vital reagents, and collected and analyzed data; J.W. and H.H. designed research, contributed vital reagents and analytical tools, and wrote the paper. A.U. and K.D. contributed equally to this work.

Conflict-of-interest disclosure: The authors declare no competing financial interests.

Correspondence: Prof Dr med Heidi Hahn, Section of Molecular Developmental Genetics, Institute of Human Genetics, University of Goettingen, Heinrich-Dueker-Weg 12, D-37073 Goettingen, Germany; e-mail: hhahn@gwdg.de; Prof Dr Jürgen Wienands, Cellular and Molecular Immunology, Georg August University Goettingen, Humboldtallee 34, 37073 Goettingen, Germany; jwienan@uni-goettingen.de.

References

- Kondo M, Weissman IL, Akashi K. Identification of clonogenic common lymphoid progenitors in mouse bone marrow. *Cell*. 1997;91:661-672.
- Akashi K, Traver D, Miyamoto T, Weissman IL. A clonogenic common myeloid progenitor that gives rise to all myeloid lineages. *Nature*. 2000;404:193-197.
- Laiosa CV, Stadtfeld M, Graf T. Determinants of lymphoid-myeloid lineage diversification. *Annu Rev Immunol*. 2006;24:705-738.
- Busslinger M. Transcriptional control of early B cell development. *Annu Rev Immunol*. 2004;22:55-79.
- Bhardwaj G, Murdoch B, Wu D, et al. Sonic hedgehog induces the proliferation of primitive human hematopoietic cells via BMP regulation. *Nat Immunol*. 2001;2:172-180.
- Trowbridge JJ, Scott MP, Bhatia M. Hedgehog modulates cell cycle regulators in stem cells to control hematopoietic regeneration. *Proc Natl Acad Sci U S A*. 2006;103:14134-14139.
- Andaloussi AE, Graves S, Meng F, Mandal M, Mashayekhi M, Aifantis I. Hedgehog signaling controls thymocyte progenitor homeostasis and differentiation in the thymus. *Nat Immunol*. 2006;7:418-426.
- Sacedon R, Diez B, Nunez V, et al. Sonic hedgehog is produced by follicular dendritic cells and protects germinal center B cells from apoptosis. *J Immunol*. 2005;174:1456-1461.
- Shah DK, Hager-Theodorides AL, Outram SV, Ross SE, Varas A, Crompton T. Reduced thymocyte development in sonic hedgehog knockout embryos. *J Immunol*. 2004;172:2296-2306.
- Outram SV, Varas A, Pepicelli CV, Crompton T. Hedgehog signaling regulates differentiation from double-negative to double-positive thymocyte. *Immunity*. 2000;13:187-197.
- Rowbotham NJ, Hager-Theodorides AL, Cebeaucuer M, et al. Activation of the Hedgehog signaling pathway in T lineage cells inhibits TCR repertoire selection in the thymus and peripheral T cell activation. *Blood*. 2007;109:3757-3766.
- Ruiz i Altaba A, Sanchez P, Dahmane N. Gli and hedgehog in cancer: tumours, embryos and stem cells. *Nat Rev Cancer*. 2002;2:361-372.
- Toftgard R. Hedgehog signalling in cancer. *Cell Mol Life Sci*. 2000;57:1720-1731.
- Chiang C, Litingtung Y, Lee E, et al. Cyclopia and defective axial patterning in mice lacking Sonic hedgehog gene function. *Nature*. 1996;383:407-413.
- Goodrich LV, Milenkovic L, Higgins KM, Scott MP. Altered neural cell fates and medulloblastoma in mouse patched mutants. *Science*. 1997;277:1109-1113.
- Hahn H, Wojnowski L, Zimmer AM, Hall J, Miller G, Zimmer A. Rhabdomyosarcomas and radiation hypersensitivity in a mouse model of Gorlin syndrome. *Nat Med*. 1998;4:619-622.
- Conrad M, Brielmeier M, Wurst W, Bornkamm GW. Optimized vector for conditional gene targeting in mouse embryonic stem cells. *Biotechniques*. 2003;34:1136-1138, 1140.
- Rodriguez CI, Buchholz F, Galloway J, et al. High-efficiency deleter mice show that FLPe is an alternative to Cre-loxP. *Nat Genet*. 2000;25:139-140.
- Nagy A, Rossant J, Nagy R, Abramow-Newerly W, Roder JC. Derivation of completely cell culture-derived mice from early-passage embryonic stem cells. *Proc Natl Acad Sci U S A*. 1993;90:8424-8428.
- Mansour SL, Thomas KR, Capecci MR. Disruption of the proto-oncogene int-2 in mouse embryo-derived stem cells: a general strategy for targeting mutations to non-selectable genes. *Nature*. 1988;336:348-352.
- Imai T, Jiang M, Chambon P, Metzger D. Impaired adipogenesis and lipolysis in the mouse upon selective ablation of the retinoid X receptor alpha mediated by a tamoxifen-inducible chimeric Cre recombinase (Cre-ERT2) in adipocytes. *Proc Natl Acad Sci U S A*. 2001;98:224-228.
- DeKoter RP, Lee HJ, Singh H. PU. 1 regulates expression of the interleukin-7 receptor in lymphoid progenitors. *Immunity*. 2002;16:297-309.
- Bhattacharya D, Rossi DJ, Bryder D, Weissman IL. Purified hematopoietic stem cell engraftment of rare niches corrects severe lymphoid deficiencies without host conditioning. *J Exp Med*. 2006;203:73-85.
- Nagao K, Togawa N, Fujii K, et al. Detecting tissue-specific alternative splicing and disease-associated aberrant splicing of the PTCH gene with exon junction microarrays. *Hum Mol Genet*. 2005;14:3379-3388.
- Kuhn R, Schwenk F, Aguet M, Rajewsky K. Inducible gene targeting in mice. *Science*. 1995;269:1427-1429.
- Bhandoola A, Sambandam A. From stem cell to T cell: one route or many? *Nature Rev Immunol*. 2006;6:117-126.
- Loder F, Mutschler B, Ray RJ, et al. B cell development in the spleen takes place in discrete steps and is determined by the quality of B cell receptor-derived signals. *J Exp Med*. 1999;190:75-89.
- Nagasawa T. Microenvironmental niches in the bone marrow required from B-cell development. *Nat Rev Immunol*. 2006;6:107-116.
- Porse BT, Bryder D, Theilgaard-Monch K, et al. Loss of C/EBP alpha cell cycle control increases myeloid progenitor proliferation and transforms the neutrophil granulocyte lineage. *J Exp Med*. 2005;202:85-96.
- Metcalf D. Stem cells, pre-progenitor cells and lineage-committed cells: are our dogmas correct?

- Ann N Y Acad Sci. 1999;872:289-303; discussion: 303-284.
31. Okada S, Nakauchi H, Nagayoshi K, Nishikawa S, Miura Y, Suda T. In vivo and in vitro stem cell function of c-kit- and Sca-1-positive murine hematopoietic cells. *Blood*. 1992;80:3044-3050.
 32. Katayama N, Shih JP, Nishikawa S, Kina T, Clark SC, Ogawa M. Stage-specific expression of c-kit protein by murine hematopoietic progenitors. *Blood*. 1993;82:2353-2360.
 33. Iwasaki H, Somoza C, Shigematsu H, et al. Distinctive and indispensable roles of PU. 1 in maintenance of hematopoietic stem cells and their differentiation. *Blood*. 2005;106:1590-1600.
 34. Smale ST, Dorshkind K. Hematopoiesis flies high with Ikaros. *Nat Immunol*. 2006;7:367-369.
 35. Wetmore C. Sonic hedgehog in normal and neoplastic proliferation: insight gained from human tumors and animal models. *Curr Opin Genet Dev*. 2003;13:34-42.
 36. Mazurier F, Fontanellas A, Salesse S, et al. A novel immunodeficient mouse model—RAG2 x common cytokine receptor gamma chain double mutants—requiring exogenous cytokine administration for human hematopoietic stem cell engraftment. *J Interferon Cytokine Res*. 1999;19:533-541.
 37. Orlic D, Girard LJ, Lee D, Anderson SM, Puck JM, Bodine DM. Interleukin-7R alpha mRNA expression increases as stem cells differentiate into T and B lymphocyte progenitors. *Exp Hematol*. 1997;25:217-222.
 38. Passegue E, Wagers AJ, Giuriato S, Anderson WC, Weissman IL. Global analysis of proliferation and cell cycle gene expression in the regulation of hematopoietic stem and progenitor cell fates. *J Exp Med*. 2005;202:1599-1611.
 39. Palmer E. Negative selection: clearing out the bad apples from the T-cell repertoire. *Nat Rev Immunol*. 2003;3:383-391.
 40. Germain RN. T-cell development and the CD4-CD8 lineage decision. *Nat Rev Immunol*. 2002;2:309-322.



blood[®]

2007 110: 1814-1823

doi:10.1182/blood-2007-02-075648 originally published
online May 29, 2007

The Hedgehog receptor Patched controls lymphoid lineage commitment

Anja Uhmann, Kai Dittmann, Frauke Nitzki, Ralf Dressel, Milena Koleva, Anke Frommhold, Arne Zibat, Claudia Binder, Ibrahim Adham, Mirko Nitsche, Tanja Heller, Victor Armstrong, Walter Schulz-Schaeffer, Jürgen Wienands and Heidi Hahn

Updated information and services can be found at:

<http://www.bloodjournal.org/content/110/6/1814.full.html>

Articles on similar topics can be found in the following Blood collections

[Hematopoiesis and Stem Cells](#) (3362 articles)

[Signal Transduction](#) (1930 articles)

Information about reproducing this article in parts or in its entirety may be found online at:

http://www.bloodjournal.org/site/misc/rights.xhtml#repub_requests

Information about ordering reprints may be found online at:

<http://www.bloodjournal.org/site/misc/rights.xhtml#reprints>

Information about subscriptions and ASH membership may be found online at:

<http://www.bloodjournal.org/site/subscriptions/index.xhtml>